
This is an electronic reprint of the original article.
This reprint may differ from the original in pagination and typographic detail.

Giblin, Stephen; Mykkanen, Emma; Kemppinen, Antti; Immonen, Pekka; Manninen, Antti; Jenei, Mate; Mottonen, Mikko; Yamahata, Gento; Fujiwara, Akira; Kataoka, Masaya
Realisation of a quantum current standard at liquid helium temperature with sub-ppm reproducibility

Published in:
Metrologia

DOI:
[10.1088/1681-7575/ab72e0](https://doi.org/10.1088/1681-7575/ab72e0)

Published: 01/04/2020

Document Version
Peer-reviewed accepted author manuscript, also known as Final accepted manuscript or Post-print

Please cite the original version:
Giblin, S., Mykkanen, E., Kemppinen, A., Immonen, P., Manninen, A., Jenei, M., Mottonen, M., Yamahata, G., Fujiwara, A., & Kataoka, M. (2020). Realisation of a quantum current standard at liquid helium temperature with sub-ppm reproducibility. *Metrologia*, 57(2), Article 025013. <https://doi.org/10.1088/1681-7575/ab72e0>

This material is protected by copyright and other intellectual property rights, and duplication or sale of all or part of any of the repository collections is not permitted, except that material may be duplicated by you for your research use or educational purposes in electronic or print form. You must obtain permission for any other use. Electronic or print copies may not be offered, whether for sale or otherwise to anyone who is not an authorised user.



PAPER

Realisation of a quantum current standard at liquid helium temperature with sub-ppm reproducibility

To cite this article: Stephen P Giblin *et al* 2020 *Metrologia* **57** 025013

View the [article online](#) for updates and enhancements.

Realisation of a quantum current standard at liquid helium temperature with sub-ppm reproducibility

Stephen P Giblin¹ , Emma Mykkänen² , Antti Kemppinen², Pekka Immonen², Antti Manninen² , Máté Jenei³, Mikko Möttönen³, Gento Yamahata⁴ , Akira Fujiwara⁴ and Masaya Kataoka¹ 

¹ National Physical Laboratory, Hampton Road, Teddington, Middlesex TW11 0LW, United Kingdom

² VTT Technical Research Centre of Finland Ltd, National Metrology Institute VTT MIKES, Espoo, FI-02044 VTT, Finland

³ QCD Labs, QTF Centre of Excellence, Department of Applied Physics, Aalto University, PO Box 13500, FI-00076 AALTO, Finland

⁴ NTT Basic Research Laboratories, NTT Corporation, 3-1 Morinosato Wakamiya, Atsugi, Kanagawa 243-0198, Japan

E-mail: stephen.giblin@npl.co.uk

Received 19 November 2019, revised 13 January 2020

Accepted for publication 4 February 2020

Published 19 March 2020



CrossMark

Abstract

A silicon electron pump operating at the temperature of liquid helium has demonstrated repeatable operation with sub-ppm accuracy. The pump current, approximately 168 pA, is measured by three laboratories, and the measurements agree with the expected current ef within the uncertainties which range from 0.2 ppm to 1.3 ppm. All the measurements are carried out in zero applied magnetic field, and the pump drive signal is a sine wave. The combination of simple operating conditions with high accuracy demonstrates the possibility that an electron pump can operate as a current standard in a National Measurement Institute. We also discuss other practical aspects of using the electron pump as a current standard, such as testing its robustness to changes in the control parameters, and using a rapid tuning procedure to locate the optimal operation point.

Supplementary material for this article is available [online](#)

Keywords: electron pump, quantised charge pumping, SI base units

(Some figures may appear in colour only in the online journal)

1. Introduction

Moving electrons one at a time is a conceptually simple and elegant way to generate an accurate reference current. Following the 2019 re-definition of the International System of Units (SI), such a method is also a most direct way to realise the SI base unit ampere [1, 2], requiring only a traceable measurement of the clock frequency f . Mesoscopic devices which aim to achieve this controlled electron transport, electron pumps and turnstiles, have been the subject of research for more than 30 years [3]. In the last 10 years, pumps based on semiconductor quantum dots have made remarkable progress

[4, 5], and devices based on silicon [6] and gallium arsenide [7] have demonstrated an accuracy approaching 1 part in 10^7 . The general metrological utility of electron pumps requires, in addition to the absolute accuracy, a broader class of properties to be demonstrated. These include reproducibility of the pump operation across multiple cool-downs, reliability of device fabrication, and operation under conditions which are accessible in a wide range of National Measurement Institutes (NMIs). A simple procedure for tuning the pump is also highly desirable. Thus far, bench-mark experiments such as those reported in references [6, 7] have required sophisticated cryogenic infrastructure; a helium-3 refrigerator [6] and a dilution

refrigerator [7]. In the case of reference [7] a high magnetic field was also applied to improve the quantisation accuracy. These types of refrigerators carry significant cost challenges, and are not widely available at NMIs. Precision measurements of a pump at the temperature of liquid helium, or on multiple cool-downs, have not yet been reported.

In this work, we address some of these practical aspects of electron pumps. A well-characterised silicon electron pump was measured by three laboratories: NPL (UK), VTT MIKES (Finland) and Aalto University (Finland), designated throughout this work as ‘NPL’, ‘MIKES’ and ‘Aalto’. At each institute, the pump current was found to agree with the ideal error-free current $Ne \times f$, where $N = 1$ is the number of electrons pumped in each cycle of the clock frequency f , within a relative uncertainty of 10^{-6} or less. Significantly, these precision measurements were performed with the pump cooled in liquid helium at a temperature of 4.2 K, and zero applied magnetic field. These experimental conditions are considerably relaxed compared to all previous precision measurements. The measurements at MIKES and Aalto were also carried out using a quick and simple tuning procedure developed at NPL, yielding precision measurements 1–2 days after cooling down the pump.

2. Device and experiment time-line

The electron pump used in this work has been previously measured [8] in 2015, when it demonstrated a pump current I_P on the $N = 1$ plateau equal to ef within a relative uncertainty of 9.2×10^{-7} . The device, illustrated schematically in figure 1, is a silicon nano-MOSFET, in which the charge carriers are induced in an undoped nano-wire by applying a positive voltage $V_{TOP} = 4$ V to a top gate [8, 9]. Negative voltages V_{ENT} and V_{EXIT} applied to two finger gates crossing the nano-wire create potential barriers and define a quantum dot in between the barriers. Ratchet-mode single-electron pumping was induced by adding an AC signal to V_{ENT} through a 3-dB attenuator and a room-temperature bias-tee. The AC pumping signal was a sine wave from an RF source with output power level denoted P_{RF} .

The 2015 measurements [8] were performed at a temperature of 1.5 K, zero applied magnetic field, and $f = 1$ GHz. In the intervening period, the device was left bonded into its NPL-designed sample holder, which was stored in an anti-static box at room temperature. In this work the device is cooled to a temperature of 4.2 K by lowering it into a dewar of liquid helium. The same NPL-designed cryogenic probe is used to cool the sample at the three laboratories, but different liquid helium cryostats (also known as dewars) are used at each laboratory, and different models of commercial instrument are used to generate the DC and AC control voltages. The DC voltages V_{ENT} , V_{EXIT} and V_{TOP} were filtered using low-pass filters (not shown in figure 1), with $2\pi RC = 14$ ms, to suppress noise from the electronic voltage sources. The same filters were used at all the laboratories. The DC wiring in the probe was of a custom design to minimise electrical noise due to vibration and triboelectric effects. Its design will be the subject of a

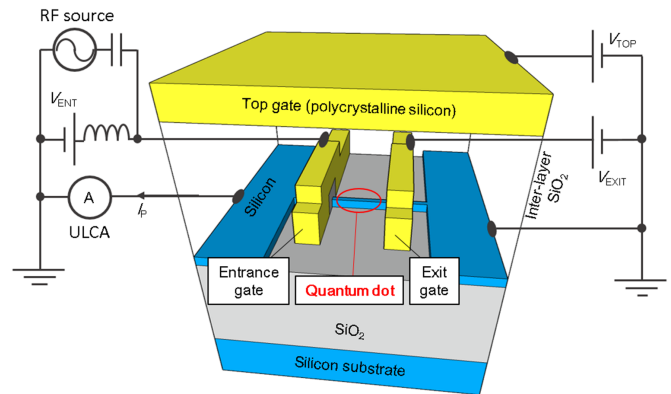


Figure 1. Schematic diagram of the electron pump device, showing the electrical connections to the device terminals. Electrons are pumped from left to right, so the ultrastable low-noise current amplifier (ULCA) connected to the left terminal measures current with a positive sign.

future paper, and is summarised in supplementary section G, available online at (stacks.iop.org/MET/57/025013/mmedia). A pumping frequency of $f = 1.05$ GHz is used for all the measurements, generating a current of $I_P \approx 168$ pA. The choice of frequency is constrained by dips in the transmission of the high-frequency wiring in the cryogenic probe.

The temporal order of the experiments is as follows: first, the stability of the pump under multiple cool-downs was evaluated at NPL. The pump was cooled down 7 times between July 2018 and February 2019, showing remarkable reproducibility. The values of V_{ENT} and V_{EXIT} for tuning the device to the one-electron plateau varied by less than 10% from one cool-down to the next. Precision measurements of the pump current were made on cool-downs 5 and 6, and data from both cool-downs is reported in this paper. During these cool-downs, the robustness of the pump current to changes in V_{ENT} and V_{EXIT} was evaluated, and a provisional tuning procedure was developed for rapidly locating the optimal values of these voltages for accurate pumping. The device was hand-carried by air to MIKES on 7th April 2019, and cooled down the next day. The rapid tuning procedure was applied, and the first precision measurements were made less than 24 hours after cooling the sample. Following a campaign of measurements at MIKES, the device was warmed up and hand-carried to Aalto (a distance of less than 1 km) on 5th May 2019. For this transportation, the device sample holder was not removed from the cryogenic probe. The tuning procedure was applied in the same way at Aalto, as at MIKES. The campaign of measurements at Aalto lasted until 3rd June.

3. Precision measurement setups

All measurements of the pump current are carried out using an ultrastable low-noise current amplifier (ULCA) [10] connected to the source side of the pump (see figure 1). This is a transresistance amplifier with nominal current-to-voltage gain $A_{TR} = 10^9$ V/A, with the key feature that this gain is very stable in time: the gain of a number of ULCA units

has been shown to be stable at the level of 1 part in 10^6 on time-scales of a year [11]. A single ULCA unit (the ‘NPL ULCA’) is used for measurements at NPL. Its gain is calibrated using the NPL high-resistance CCC [12]. A second ULCA unit (the ‘MIKES ULCA’) is used for measurements at MIKES and Aalto. Its gain is calibrated at MIKES using a Magnicon CCC. The ULCA was transported between MIKES and Aalto by car. Although the temperature of the ULCA was not logged during these short transportations, they took place during a warm time of year. Shifts in the ULCA gain which have been observed when the ULCA is exposed to low temperatures during transportation [11, 12] are not expected to be a problem here. More detailed information about the ULCA calibrations can be found in the supplementary information, section B.

The output voltage of the ULCA is digitised by a precision digital voltmeter (DVM). All three laboratories used a Hewlett Packard / Agilent / Keysight 3458A for this function¹. The DVM is set to integrate each data point for 10 power line cycles (PLC), with an auto zero operation every 20 data points. The Optimisation of the DVM auto zero is discussed in reference [7]. Each laboratory uses a different DVM unit. All DVMs are calibrated with traceability to a Josephson voltage standard (JVS), but the exact traceability routes are different. At NPL, the DVM is calibrated directly against a JVS using an automated switch with a calibration interval of approximately an hour. At MIKES, some calibrations are carried out directly against the JVS, and some using an intermediate 1-V Zener voltage standard. The minimum calibration interval is approximately a day. At Aalto, all calibrations are carried out using a Zener voltage standard calibrated against the JVS at MIKES and hand-carried to Aalto. This resulted in a higher uncertainty contribution due to the DVM calibration at Aalto, shown in table 1.

In this paper we present two types of data: for ‘standard precision’ data, the ULCA output voltage is recorded as a pump parameter such as a gate voltage is scanned. This type of data is used for characterisation of the pump. For ‘high precision’ data, as in previous studies, the pump is turned on and off, and I_P is extracted from the on-off difference signal to eliminate possible instrumental offset drift from the data. Two types of on-off cycle are used in this work. In the ‘power switching’ cycle, the AC drive signal at the entrance gate is turned on and off. This is how all previous precision pump measurements have been carried out [5], although here we use a longer on-off cycle than typically used in the past: 1000 data points (228 seconds) per on or off segment at NPL and MIKES, 1300 points (296 seconds) per segment at Aalto. The first 300 points were rejected from each data segment prior to analysis, to avoid time constant effects. Note that the time given for each segment includes the time required for the auto zero operations. In the ‘gate switching’ cycle, the AC drive is left on, and V_{EXIT} is stepped from its operation point to -1.7 V, well into the $N=0$ region of the pump map. This type of cycle avoids

Table 1. Breakdown of the uncertainty components for the five long high-precision measurements shown in figure 4. All entries in the table are dimensionless relative uncertainties ($k=1$) in parts per million. The largest uncertainty contribution for each measurement is highlighted in bold type.

Contribution	NPL 1	NPL 2	MIKES 1	MIKES 2	Aalto
ULCA G_I Calibration	0.023	0.031	0.035	0.044	0.044
ULCA R_{IV} Calibration	0.056	0.056	0.065	0.066	0.066
ULCA G_I Drift	0.014	0.014	0.044	0.074	0.074
ULCA R_{IV} Drift	0.019	0.019	0.018	0.042	0.042
Voltmeter Calibration	0	0	0.17	0.18	1.20
Voltmeter Drift	0	0	0.18	0.046	0.38
Leakage correction	0	0.40	0	0.30	0
Pump measurement	0.20	0.14	0.137	0.17	0.25
type A					
Total	0.21	0.43	0.30	0.41	1.30

time constants possibly due to RF heating (see supplementary section D) but I_P has to be corrected for the change in leakage current due to stepping the gate voltage. This correction is also detailed in the supplementary information, section E. As shown in table 1, the uncertainty in the leakage correction is the largest contribution to the combined uncertainty in the measurements using the gate switching cycle.

A note on the data analysis: Our main results are reported as dimensionless numbers, the fractional deviation of the pump current from ef : $\Delta I_P = (I_P - ef)/(ef)$, and are therefore independent of the choice of unit system. Since the experiments pre-date the May 2019 redefinition of the SI, we chose to analyse the precision measurements within the system of 1990 electrical units: The calibration of the ULCA gain is traced to the quantum Hall resistance using R_{K-90} , the voltmeters are calibrated with reference to K_{J-90} , and we report the deviation of the pump current from $f \times e_{90}$, where $e_{90} \equiv 2/(K_{J-90}R_{K-90})$. The constants R_{K-90} and K_{J-90} are the fixed values assigned to the von Klitzing and Josephson constants respectively in 1990. They were used for representing the SI ohm and volt from then until the 2019 redefinition.

4. Characterisation and tuning

After cooling down the device in liquid helium, the first stage of characterisation is to record a pump map. In figure 2, we present differential pump current maps measured at the three laboratories. The pump map is a standard fingerprint for a tunable-barrier pump, which shows the ranges of V_{ENT} and V_{EXIT} where the current is quantised (white areas) and the transitions between quantised plateaus (black lines). The characteristic pattern of quantised current regions establishes that the pump is operating in a ratchet mode [13]. The similarity between the three pump maps shows the stability of the pump after thermal cycling and transportation, but some small differences are visible. Despite a higher RF generator power, the pump map measured at MIKES is not as extended along the V_{ENT} axis as the map measured at NPL, indicating a lower AC voltage present on the entrance gate. Similar behaviour has

¹ Mention of specific models of commercial instrument is for information only and does not imply endorsement by the authors or their respective institutions.

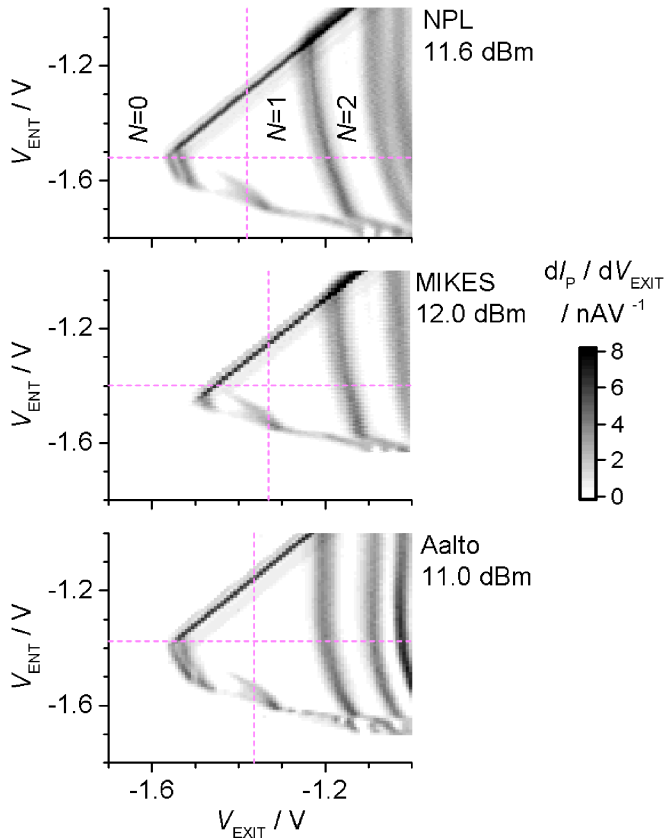


Figure 2. Derivative of the pump current with respect to exit gate voltage, as a function of entrance and exit gate voltages, measured at NPL, MIKES, and Aalto. The number of electrons pumped per cycle, N , is indicated in the first three plateau regions of the top-most panel. The laboratory identifier and RF generator output power P_{RF} are indicated next to each panel. The data of figure 3 was taken along the cuts indicated by the horizontal and vertical dashed lines.

also been observed during multiple cool-downs at NPL. This variation may be due to two processes: firstly, small changes in carrier concentration of the sample and secondly, changes in the reflection co-efficients at connectors in the coaxial RF transmission line. The latter is a plausible mechanism, as the properties of the RF connectors are sensitive to mechanical strain induced by the large temperature gradient along the transmission line. The pump occasionally switched to a different state characterised by a wider pump map along the entrance gate axis, as detailed in supplementary section F. None of the measurements reported in the paper were carried out in this state.

Next, the extent of the quantised current region is estimated by studying the deviation of I_p from ef on a logarithmic scale [14], in figure 3, along the line cuts indicated by dotted lines on the pump maps of figure 2. The fixed values of V_{ENT} and V_{EXIT} for these line cuts are established from a few iterations of plotting data similar to figure 3, starting from initial guesses, and adjusting V_{ENT} and V_{EXIT} with each iteration to maximise the plateau width. The exponential approaches to the plateau can be extrapolated (dash-dot lines) to predict the extent of the plateau at the 0.1 ppm accuracy level. At NPL, high-precision scans (open and closed pink triangles) were

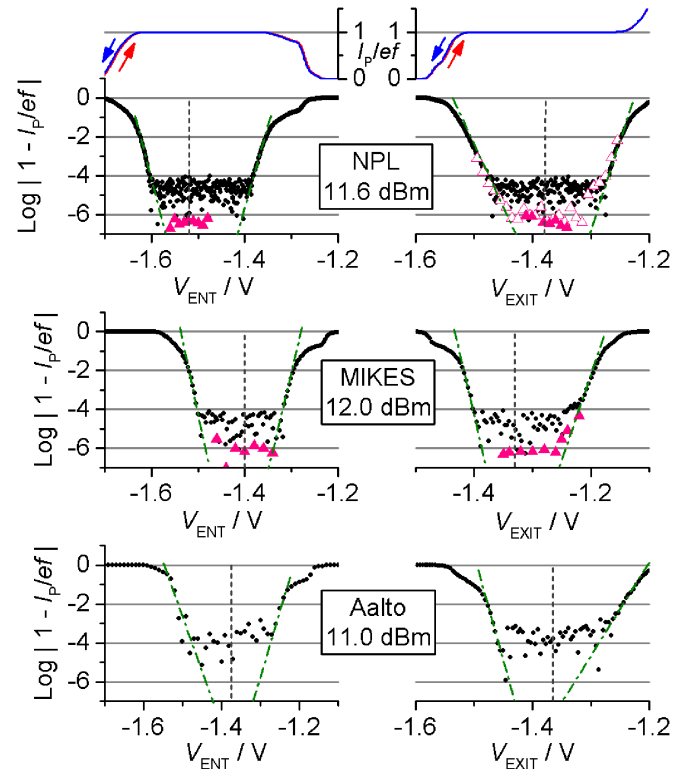


Figure 3. The 6 main plots show relative deviation of the pump current from the expected value $e \times f$ along the V_{ENT} and V_{EXIT} axes indicated by the dashed lines in figure 2. Black circles: Standard precision data, where each data point is a single 10 PLC measurement. Data was taken by sweeping the voltages from negative to positive (left to right along the x-axis). The dash-dot lines are guides to the eye for the exponential approaches to the $N = 1$ plateau. Open and closed pink triangles: High-precision data, where each data point is extracted from a number of on-off cycles. The laboratory identifier and RF generator power P_{RF} are indicated next to each pair of plots. Vertical dashed lines indicate the values of V_{ENT} and V_{EXIT} selected for the high-precision measurements presented in figure 4. The two small plots at the top of the figure show the NPL standard-precision data on linear y-axes (red lines), together with additional data (blue lines) taken with the sweep direction reversed.

carried out to verify the flatness of the plateaus at the 1-ppm level, before selecting an operation point, $V_{ENT} = -1.52$ V and $V_{EXIT} = -1.38$ V, indicated by the vertical dashed lines. At MIKES and Aalto, the emphasis is on a quick characterisation procedure, and operation points are chosen based solely on standard-precision data. A certain amount of subjective judgment entered into the selection of these operation points. For example, the exit gate scan at MIKES seems to indicate a shoulder, only just resolved by the black data points, at $V_{EXIT} \sim -1.25$ V. This feature biases the selection of the operation point towards more negative V_{EXIT} . The feature does not appear in the high-precision scan (pink triangles), but this scan was measured after the long high-precision measurements shown in figure 4, and did not play a role in the selection of the operation point. We also checked that the location of the plateau was not biased by the finite scan rate of the gate voltage combined with possible hysteresis, by comparing scans with opposite scan directions. Two such pairs

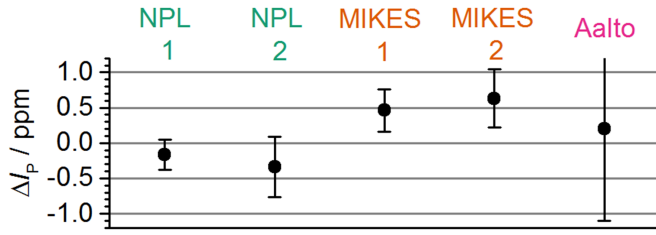


Figure 4. Results of long high-precision measurements at fixed gate voltages, expressed as the dimensionless deviation of the pump current from $e_{90}f$. Error bars are combined standard uncertainties ($k = 1$). Entrance and exit gate voltages for the data points ‘NPL 1’, ‘MIKES 1’ and ‘Aalto’ are shown by the intersections of the dashed lines in figure 2. data points ‘NPL 2’ and ‘MIKES 2’ were taken at slightly different gate voltages following a repeat of the tuning procedure.

of scans are shown above the NPL log-scale plots, with the same x-axis scales and linear y-axes, showing negligible hysteresis.

5. High-precision measurements

At each laboratory, several high-precision measurements are carried out at the optimal operation points determined from figure 3. These measurements are typically carried out overnight, with averaging times from 10 to 22 hours. Results from five of them are shown in figure 4, in terms of the dimensionless deviation of the pump current from $e_{90}f$, $\Delta I_P = (I_P - e_{90}f)/(e_{90}f)$. Measurements denoted NPL 1, MIKES 1, and Aalto utilise the power switching on-off cycle, and measurements NPL 2 and MIKES 2 utilise the gate switching cycle. Error bars indicate the combined standard ($k = 1$) uncertainty.

The breakdown of the uncertainties is detailed in table 1. We have distinguished the uncertainties due to the two separate stages of calibrating the ULCA: The input current gain stage G_I , and the output trans-resistance stage R_{IV} . At NPL, the DVM calibrations are interleaved with the pump measurements, so that the uncertainty in these calibrations does not appear as separate terms: instead it is combined into the type A uncertainty as detailed in supplementary section C. At MIKES and Aalto, the DVM calibrations performed before and after the pump measurement give separate uncertainty contributions due to DVM calibration uncertainty and drift. The leakage correction, described in supplementary section E, only contributes an uncertainty to measurements using the gate-switching on-off cycle. Terms contributing a relative uncertainty less than 10^{-8} , for example the uncertainty in the pump frequency f , have been neglected from the analysis.

6. Plateau robustness

In recent years, there has been discussion [2, 5] about the possible form of guidelines for testing the accuracy of single electron pumps, in analogy to the guidelines for quantum Hall

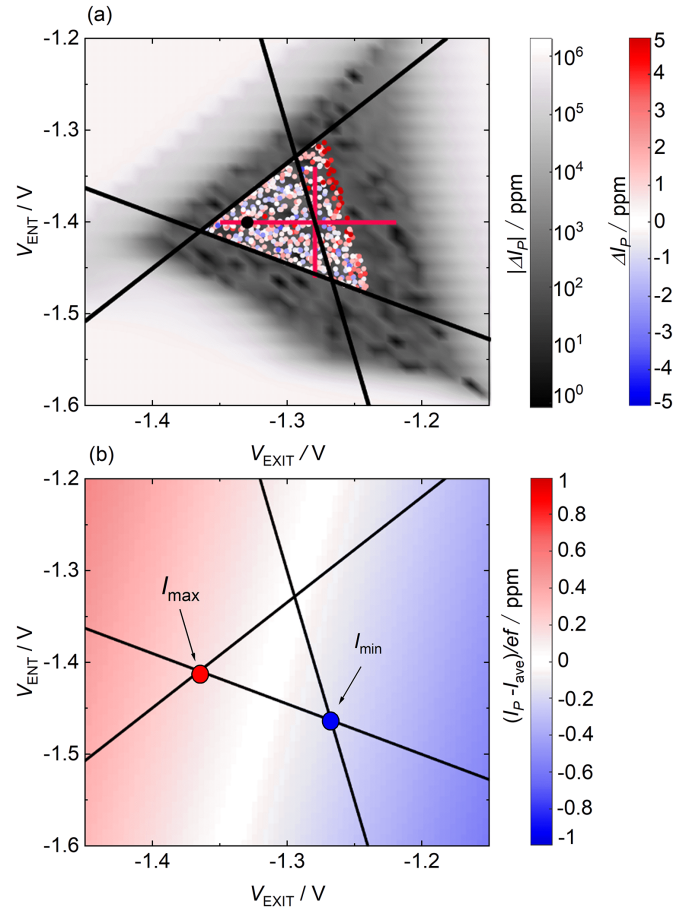


Figure 5. Method for studying the robustness of single-electron pumps. The triangular data range used for the multiple-linear-regression fit is shown by the black lines. (a) Standard precision data of the quantized current plateau is shown on greyscale. Randomized high-precision current measurement data are shown by coloured dots. The magenta lines show the parameter regime where the traceable MIKES data of figure 3 are measured. The black dot shows where the precision measurement of figure 4 was carried out. (b) The results of the multiple-linear-regression analysis of the current plateau inside the triangular area between the black lines. The deviation of the fitted plane from average value $I_{ave} = (I_{max} + I_{min})/2$ is plotted using a colour code to illustrate the small tilt of the fit plane. I_{max} and I_{min} are the maximum and minimum values of the fitted currents inside the fit area, respectively.

resistance standards [15]. A key conclusion is that a candidate single-electron-based quantum current standard should demonstrate robustness of the pump current. This means that the current is independent of all control parameters within a parameter space that is experimentally feasible. The control parameters include (but are not limited to) DC gate voltages, and RF power. Experimental feasibility means that the control parameters do not have to be tuned with an unreasonably high level of precision, and that fluctuations in the tuning parameters, for example due to the imperfections of electronic sources, do not significantly change the output current.

The typical method for testing robustness, used in several studies thus far [6, 7, 14], reviewed in reference [5] and also shown in figure 3, is to find an optimal operation point and

then vary the control parameters one at a time while carrying out traceable precision measurements. This method has two main limitations. Firstly, it measures the robustness along lines in a multidimensional parameter space, which samples only a small fraction of the total parameter space. Secondly, it is also typical practice to collect the data in sequential order, incrementing the stepped control parameter from its minimum value to its maximum value. Sequential stepping has the problem that any time correlation of the measurement data (for example, caused by a drift in the calibration factor of the ULCA or DVM) will yield a spurious parameter space correlation of the data. Here, we investigated a technique which avoids these two limitations.

In figure 5, we present colour-map data of the plateau flatness in the two-dimensional parameter space defined by V_{ENT} and V_{EXIT} . Each coloured dot is the result of a single on-off cycle using the power switching method described in section 3. The values of V_{ENT} and V_{EXIT} for each data point are selected randomly, with the constraint that they should lie within a triangular region which, on a coarse scale, defines the plateau. Our measurement scheme can be generalized to all control parameters, but these two enable us to demonstrate the method.

The measurement of figure 5 took 149 hours. Neither the voltmeter nor the ULCA were calibrated during this time, so the measurement is not traceable. However, in this experiment we are only concerned with the flatness of the plateau, not its absolute value. From past experience, we expect the gain of the voltmeter to drift by up to 1 ppm on the time scale of the measurement, but we cannot make any assumptions about the magnitude or frequency spectrum of the drift. The key point is that any changes in the gain of the measurement system, whether correlated in time or not, will appear as uncorrelated fluctuations along the V_{ENT} and V_{EXIT} axes and will be indistinguishable from fluctuations due to random noise. The effect of the changes in measurement system gain will be to increase the uncertainty in the fitted plateau slope, but the value of the fitted slope itself will only contain information about dependence of the pump current on V_{ENT} and V_{EXIT} .

Linear regression analysis (fitting a plane to a 2-dimensional data set) was performed on a subset of the precision data of figure 5(a), bounded by the thick black lines in the figure. The data subset was chosen to avoid the clear increase in the pump current at the right of the plot. The standard deviation of the data points used for the fit is 1.5 ppm. The fitted control parameter dependencies of I_{P} are (-3.0 ± 4.3) ppm/V and (0.5 ± 3.2) ppm/V for V_{EXIT} and V_{ENT} , respectively. The plateau tilt $\Delta I = I_{\text{max}} - I_{\text{min}} = (0.3 \pm 0.5)$ ppm. This numerical statement about the plateau flatness is essentially a 2-dimensional extension of earlier attempts to define the pump plateau as the range of data points in a one-dimensional scan for which the uncertainty in the gradient of a linear fit is greater than the fitted gradient [14]. In this work, unlike in reference [14], we have randomised the order of the data points which means that drift in the calibration of the measuring instruments only increases the random scatter of the data points (and therefore the uncertainty in the fitted slope), but cannot be mistaken for a sloped plateau. We find that there

is thus no tilt of the plateau within the measurement uncertainty. Finally, we want to point out that in a more optimized measurement protocol, which does not include zero measurements or too many points outside the accurate plateau, a similar uncertainty for the robustness can be obtained in a few days.

7. Discussion

The electron pump used in this study displayed, overall, a remarkable level of stability over many cooldowns and handling procedures. The stability of Coulomb blockade features of silicon single-electron devices is already well-known [16, 17], and we discovered that this stability carries onto high-precision electron pumping. The measurements at MIKES and Aalto showed that a rapid characterisation procedure could yield a pump current accurate to a part per million, on a measurement time-scale of roughly 2 days. This is comparable to the time required for basic checks on a quantum Hall resistance sample [15] prior to using it as a primary resistance standard. The tuning procedure detailed in section 4 was empirically developed based on approximately 3 weeks of measurement data taken at NPL. We are not proposing it as a universal method for tuning an electron pump, but our data provide encouraging evidence that such a universal and useful method may be developed.

The accurate operation of the pump at a temperature of 4 K is one of the key findings of this study. This is due to the large addition energy of the silicon nanowire quantum dot. We did not estimate the addition energy for our particular device, but recent measurements of a similar device resulted in an estimate $E_{\text{add}} = 12$ meV [18], corresponding to a characteristic temperature $E_{\text{add}}/k_{\text{B}} = 140$ K. The large addition energy for the silicon nanowire pumps is also shown by the presence of current plateaus, in a similar device to the one used in this study, at a temperature of 20 K and $f = 2.3$ GHz [9]. In contrast, typical GaAs quantum dots have charging energies in the range 1 to 2 meV [19], and the most accurate measurements on these pumps have been done in a dilution refrigerator at temperatures of 0.1 K [7, 20]. In previous studies, fits to the $I_{\text{P}}(V_{\text{EXIT}})$ data have determined whether back-tunneling [14], or thermal exchange of electrons with the source lead [6] was the dominant mechanism in determining the number of electrons pumped in each cycle. It was not possible to extract this information for the device in this study, because of the anomalous transition from pumping zero to one electrons, clearly visible as the double line at the ‘nose’ of the NPL derivative pump map in figure 2. Further studies will investigate the pumping mechanism, as well as probing the upper frequency limit for accurate pumping.

The MIKES results on the pump current are above ef by marginally more than a standard deviation. This offset is on the border of statistical significance, but it is noteworthy that it appears in both the MIKES 1 and MIKES 2 runs, which employed different types of on-off cycling, and in other precision measurements at different operation points (not shown) made during this cool-down at MIKES. Thus the offset is

unlikely to be due to an error in the leakage current correction, which would affect MIKES 2 only. It is also unlikely to be due to an error in the voltmeter calibration, as the measurement runs were spanned by several voltmeter calibrations, some directly against a Josephson array and some using a Zener standard. The cause of the offset is under investigation. One possibility is an error in the gain of the MIKES ULCA. The calibration history of the input current gain G_1 of the MIKES ULCA shows steplike changes with relative magnitude larger than 0.2 ppm (see supplementary section B). Such changes in between the ULCA calibration and the pump current measurements would directly affect the measurement results. If this was the case, the Aalto measurements, which used the same ULCA unit, would also be offset, but the larger uncertainty in the Aalto measurements due to the DVM calibration means that the offset cannot be resolved. Another possibility is an error in the calibration of the ULCA output stage gain R_{IV} which has a nominal value of 1 M Ω . It is unlikely that a 0.5 ppm error would appear in CCC-based traceability to 1 M Ω , but a bilateral comparison of stable standard resistors such as the one reported in reference [12] could resolve this question.

All the presented results were obtained on a single device, which was extensively characterised and the subject of earlier precision measurements [8]. At the time this study was conceived, this device was the most promising one available for operation at liquid helium temperature, although some other devices showed similar pumping characteristics in characterisation measurements. Improving the yield of fabrication processes such that devices with good performance become readily available is clearly an important problem which requires further work. Some progress has already been made: for GaAs quantum dots, a recent systematic study has established clear correlations between fabrication geometry and quantum dot properties such as the charging energy [19]. This study did not investigate pumping, only static quantum dot properties accessible from DC measurements. The authors are not aware of any analogous study for silicon devices. Most groups working in the field report anecdotally that there is considerable variation in pumping performance from a batch of devices with nominally identical fabrication properties, although no systematic study has yet been published on this subject. It will be an important direction for future work.

8. Conclusions

We have reported measurements of the same electron pump at three different institutes, with uncertainties of roughly a part per million or less. All three sets of measurements are broadly in agreement with the ideal error-free current ef within the uncertainty. These are the first traceable high-precision measurements of an electron pump at the relatively high temperature of liquid helium, and they demonstrate that a well-characterised electron pump can operate as low-current reference standard using resources (a liquid helium dewar, RF sine wave synthesiser, DC voltage sources and a frequency reference) commonly available in National Measurement Institutes.

Acknowledgments

This research was supported by the UK department for Business, Energy and Industrial Strategy and the EMPIR Joint Research Project ‘e-SI-Amp’ (15SIB08). The European Metrology Programme for Innovation and Research (EMPIR) is co-financed by the Participating States and from the European Union’s Horizon 2020 research and innovation programme. M M and M J acknowledge the Academy of Finland for funding through its Centre of Excellence in Quantum Technology (QTF), project no. 312300. A F and G Y are supported by JSPS KAKENHI Grant Number JP18H05258.

ORCID iDs

Stephen P Giblin  <https://orcid.org/0000-0001-5667-5005>
 Emma Mykkänen  <https://orcid.org/0000-0001-8099-4831>
 Antti Manninen  <https://orcid.org/0000-0002-6333-3596>
 Gento Yamahata  <https://orcid.org/0000-0002-2164-2796>
 Masaya Kataoka  <https://orcid.org/0000-0001-5780-6871>

References

- [1] Kaneko N-H, Nakamura S and Okazaki Y 2016 A review of the quantum current standard *Meas. Sci. Technol.* **27** 032001
- [2] Scherer H and Schumacher H W 2019 Single-electron pumps and quantum current metrology in the revised SI *Ann. Phys. Lpz.* **1800371**
- [3] Pekola J P, Saira O-P, Maisi V F, Kemppinen A, Möttönen M, Pashkin Y A and Averin D V 2013 Single-electron current sources: Toward a refined definition of the ampere *Rev. Mod. Phys.* **85** 1421
- [4] Kaestner B and Kashcheyevs V 2015 Non-adiabatic quantized charge pumping with tunable-barrier quantum dots: a review of current progress *Rep. Prog. Phys.* **78** 103901
- [5] Giblin S, Fujiwara A, Yamahata G, Bae M-H, Kim N, Rossi A, Möttönen M and Kataoka M 2019 Evidence for universality of tunable-barrier electron pumps *Metrologia* **56** 044004
- [6] Zhao R, Rossi A, Giblin S, Fletcher J, Hudson F, Möttönen M, Kataoka M and Dzurak A 2017 Thermal-error regime in high-accuracy gigahertz single-electron pumping *Phys. Rev. Appl.* **8** 044021
- [7] Stein F et al 2017 Robustness of single-electron pumps at sub-ppm current accuracy level *Metrologia* **54** S1
- [8] Yamahata G, Giblin S P, Kataoka M, Karasawa T and Fujiwara A 2016 Gigahertz single-electron pumping in silicon with an accuracy better than 9.2 parts in 10^7 *Appl. Phys. Lett.* **109** 013101
- [9] Fujiwara A, Nishiguchi K and Ono Y 2008 Nanoampere charge pump by single-electron ratchet using silicon nanowire metal-oxide-semiconductor field-effect transistor *Appl. Phys. Lett.* **92** 042102
- [10] Drung D, Krause C, Becker U, Scherer H and Ahlers F J 2015 Ultraprecise low-noise current amplifier: A novel device for measuring small electric currents with high accuracy *Rev. Sci. Instrum.* **86** 024703
- [11] Krause C, Drung D, Götz M and Scherer H 2019 Noise-optimized ultraprecise low-noise current amplifier *Rev. Sci. Instrum.* **90** 014706
- [12] Giblin S P, Drung D, Götz M and Scherer H 2019 Interlaboratory nanoamp current comparison with

- subpart-per-million uncertainty *IEEE Trans. Instrum. Meas.* **68** 1996–2002
- [13] Kaestner B, Kashcheyevs V, Hein G, Pierz K, Siegner U and Schumacher H W 2008 Robust single-parameter quantized charge pumping *Appl. Phys. Lett.* **92** 192106
- [14] Giblin S, Bae M, Kim N, Ahn Y-H and Kataoka M 2017 Robust operation of a gallium arsenide tunable barrier electron pump *Metrologia* **54** 299
- [15] Delahaye F and Jeckelmann B 2003 Revised technical guidelines for reliable dc measurements of the quantized Hall resistance *Metrologia* **40** 217
- [16] Zimmerman N M, Huber W H, Fujiwara A and Takahashi Y 2001 Excellent charge offset stability in a si-based single-electron tunneling transistor *Appl. Phys. Lett.* **79** 3188–90
- [17] Hourdakis E, Wahl J A and Zimmerman N M 2008 Lack of charge offset drift is a robust property of si single electron transistors *Appl. Phys. Lett.* **92** 062102
- [18] Yamahata G, Ryu S, Johnson N, Sim H-S, Fujiwara A and Kataoka M 2019 Picosecond coherent electron motion in a silicon single-electron source *J. Nat. Nanotechnol.* **14** 1019–23
- [19] Gerster T et al 2019 Robust formation of quantum dots in gaas/algaas heterostructures for single-electron metrology *Metrologia* **56** 014002
- [20] Stein F et al 2015 Validation of a quantized-current source with 0.2 ppm uncertainty *Appl. Phys. Lett.* **107** 103501
- [21] Giblin S P, Kataoka M, Fletcher J D, See P, Janssen T, Griffiths J P, Jones G A C, Farrer I and Ritchie D A 2012 Towards a quantum representation of the ampere using single electron pumps *Nat. Commun.* **3** 930
- [22] Bae M-H, Ahn Y-H, Seo M, Chung Y, Fletcher J D, Giblin S P, Kataoka M and Kim N 2015 Precision measurement of a potential-profile tunable single-electron pump *Metrologia* **52** 195